THE ASTROPHYSICAL JOURNAL, 212:141–148, 1977 February 15

THE SURFACE MAGNETIC FIELD DISTRIBUTIONS OF 53 CAMELOPARDALIS AND α^2 CANUM VENATICORUM

ERMANNO F. BORRA
Département de Physique, Université Laval
AND
J. D. LANDSTREET
Department of Astronomy, University of Western Ontario
Received 1976 July 12

ABSTRACT

Effective magnetic field curves for the magnetic Ap stars 53 Cam and α^2 CVn have been obtained using a photoelectric Balmer-line magnetograph. These observations do not show the strong anharmonic behavior found in the magnetic curves of these stars as determined by photographic field measurement. The photoelectric magnetic curves are fitted very satisfactorily by oblique rotator models with modestly decentered magnetic dipole geometries. The data suggest that the anharmonic effective field curves obtained photographically for these stars arise mainly because of the difficulty of visually measuring the separation of the centroids of the right and left circularly analyzed line profiles, as suggested by Borra, although nonuniform distribution of the metals may also contribute significant effects in α^2 CVn.

Subject headings: stars: individual — stars: magnetic — stars: peculiar A — Zeeman effect

I. INTRODUCTION

In recent years it has become clear that the variations in magnetic field strength observed in many of the peculiar A stars (cf. Babcock 1960) are the result of magnetic field geometries which are not symmetric about the stellar rotation axis, and which present varying aspects as the star rotates (Preston 1971*a*). From the observed variation in field strength it is possible to infer the distribution of magnetic flux over the stellar surface, although not always uniquely.

For most known magnetic stars only the intensity-weighted average over the visible hemisphere of the components of the magnetic field along the line of sight (the effective field, H_e) has been measured as a function of phase ϕ. The curves $H_e(\phi)$ usually have approximately the form of sine waves offset from zero. Stibbs (1950) showed that such curves arise if the field geometry is that of a magnetic dipole located at the center of the star, with its axis inclined at an angle β to the rotation axis, which is seen at varying aspects as the star rotates. However, because the model involves three parameters (i, the inclination of the rotation axis to the line of sight; β; and H_p, the field strength at the pole) while essentially only two observational quantities (say, H_e^+ and H_e^-, the values of H_e at the most positive and most negative extrema of the magnetic curve) are available for fitting, the model is not unique unless i can be determined independently. An approximate value of i may sometimes be obtained from

$$\sin i = (Pv_e \sin i)/(50.6R)\,, \qquad (1)$$

where P is the rotation period in days, v_e is the stellar equatorial rotation velocity in km s^{-1}, and R is the stellar radius in solar units. However, the gradual increase in R by approximately a factor 2 during the main-sequence evolution of the star usually renders the i so determined somewhat uncertain. Magnetic broadening can also make the accurate determination of $v_e \sin i$ difficult.

The stars 53 Cam and α^2 CVn have photographically observed magnetic curves (Babcock 1960) which are quite anharmonic, and their magnetic geometries may not be closely approximated by the oblique dipole rotator model. Landstreet (1970) argued that these two stars have one magnetic pole stronger than the other. [Although Landstreet assumed that the photographically observed $H_e(\phi)$ curves are the true $H_e(\phi)$ curves for the stars, his argument is still correct as long as the H_e measured photographically refers to uniformly distributed material and is a reasonable, unique function of the surface field distribution.] A field geometry which has this property and is easy to model is obtained by displacing a dipole along its axis by a fraction a of the stellar radius. Landstreet found that the observed magnetic curves of α^2 CVn and 53 Cam could be modeled in this way, although an extremely large displacement ($a = 0.67$) was needed to reproduce the $H_e(\phi)$ curve of 53 Cam. The addition of another model parameter, a, makes the problem of uniqueness still more severe.

Preston (1969, 1970, 1971*b*) discovered that resolved Zeeman patterns could be observed in the spectra of a number of the magnetic stars, making possible the determination of the intensity-weighted average of the

total magnetic field (the mean surface field, H_s) as a function of phase. Such a curve adds two more observational parameters (say, H_s^+ and H_s^-, the extreme values observed for H_s), so that the four parameters of a displaced dipole model are uniquely determined (apart from an interchange of the values of i and β) for a star having measured H_e and H_s curves, even without prior constraints on i. Reasonably satisfactory decentered-dipole models were found for HD 126515 (Preston 1970) with $a = 0.36$, and for β CrB (Wolff and Wolff 1970) with $a = 0.1$, although the model of β CrB does not reproduce closely the narrow negative extremum observed for H_e. Huchra (1972) showed that this problem is even more severe for 53 Cam; the H_s curve he determined requires a small value of a (~ 0.15), but then the anharmonic variation of the H_e curve is not reproduced at all. However, all three of these stars have H_s curves which vary in a single wave while H_e reverses, indicating precisely the lack of symmetry which is modeled by the decentered dipole, so that it was not clear how to improve the models.

A way of resolving this problem was suggested by Borra (1974*b*: Paper I), who showed that the anharmonic variations found in 53 Cam, α^2 CVn, and β CrB may be primarily artifacts of the photographic magnetic field measuring technique. The difficulty arises essentially because of a tendency of the observer to emphasize the line cores in measuring Zeeman displacements, especially when the line profiles are complex, as at crossover. Borra found that the anharmonic magnetic curves observed for stars such as α^2 CVn and 53 Cam do require an asymmetric field distribution such as the decentered dipole, but that a marked anharmonic component should appear in photographically observed magnetic curves even for a small amount of asymmetry ($a \approx 0.1$–0.2). He suggested that this proposal could be tested with photoelectric magnetic field measurements made using the Balmer lines, which should give H_e curves that are more nearly sinusoidal than those obtained from photographic field measurements based on metal lines.

In this paper, we present new H_e curves for 53 Cam and α^2 CVn which were obtained with a Balmer-line magnetograph technique. These curves are used to derive improved magnetic models and to reexamine the validity of the decentered-dipole geometry.

II. OBSERVATIONS

The observations reported in this paper were obtained using a two-channel photoelectric Pockels cell polarimeter similar to the one described by Angel and Landstreet (1970) on the 1.5 m telescopes at Mount Palomar and Mount Wilson Observatories and the 1.2 m telescope of the University of Western Ontario. The polarimeter is used as a Balmer-line magnetograph measuring the circular polarization in the wings of Hβ which arises from the Zeeman effect when a longitudinal magnetic field is present in the star. This technique has been discussed by Landstreet *et al.* (1975) and Borra and Landstreet (1975). Circular polarization is measured in bands of 5 Å half-power bandwidth (HPBW) located at about 4.5 Å on either side of the line core, which are isolated using tilt-scanned interference filters. The polarization is measured with the filters for both channels set alternately on the longward and shortward wings of the line. Single integrations on one line wing last typically 10 minutes, and a complete observation takes 1–2 hours. The polarizations V_r and V_b measured in the longward and shortward line wings are then combined into a mean polarization $\langle V \rangle = (V_r - V_b)/2$, where $\langle V \rangle$ is related to the effective magnetic field by

$$\langle V \rangle = 4.67 \times 10^{-13} z H_e \lambda^2 (dI/d\lambda)/I , \qquad (2)$$

$I(\lambda)$ is the observed line profile, and z is the Landé factor for the line ($z = 1.0$ for the Balmer lines). All polarization measurements and their standard errors are converted to field strength measurements using equation (2). The line profile $I(\lambda)$ is measured by using the polarimeter as a two-channel ratio-mode line profile scanner, holding one interference filter fixed while the other is tilted through a series of positions covering a range of ~ 40 Å. For Hβ observations of 53 Cam and α^2 CVn, equation (1) reduces to

$$H_e(\text{gauss}) = 1.3 \times 10^4 \langle V \rangle (\%) . \qquad (3)$$

Standard errors for the polarization measurements are determined from counting statistics. These are rather small, typically lying between 0.004% and 0.04% for the measurements presented here. To confirm that they are realistic, the rms scatter s of single integrations of V_r and $-V_b$ around the mean value of $\langle V \rangle$ was calculated for each observation and compared with the scatter σ expected from counting statistics. In general $s \leqslant 1.5\,\sigma$; in the few cases where s is greater we apparently had electronic difficulties and the data were discarded. In addition, several observations of normal upper main-sequence stars, presumably nonmagnetic, showed no significant fields within the errors, which were typically 0.005% to 0.01%. We therefore conclude that the signal-to-noise ratio of our data is probably realistic.

The conversion of polarization to field strength with equation (2) is somewhat uncertain mainly because of imprecise knowledge of the line profile $I(\lambda)$. The transmission profile of an interference filter changes slightly as it is tipped. This effect becomes significant at a tilt of several degrees, and the value of $I(\lambda)$ determined in the shortward wing of Hβ is slightly different for our two Hβ filters. We estimate that the uncertainty in the conversion of $\langle V \rangle$ to H_e is of the order of 10%, comparable to our signal-to-noise ratio. However, we were careful to preserve the same instrumental system throughout the series of measurements, especially the wavelength separation of the bands in which V_r and V_b are measured, so that the *shapes* of the magnetic curves should be as accurate as the error bars indicate, even though the scale of the field is uncertain by perhaps 10%.

The observational data are presented in Tables 1 (53 Cam) and 2 (α^2 CVn). The data are in three columns

TABLE 1

Hβ MAGNETOGRAPH OBSERVATIONS OF 53 CAMELOPARDALIS

JD (2,442,000+)	$H_e + \sigma_H$ (gauss)	ϕ
495.75	+3900 ± 420	0.251
496.69	+4300 ± 460	0.368
498.66	−1900 ± 390	0.614
498.89	−3300 ± 600	0.643
500.65	−4900 ± 440	0.862
500.83	−3900 ± 420	0.884
501.65	−2100 ± 360	0.986
501.83	−1600 ± 440	0.009
502.72	+2400 ± 460	0.120
555.66	−5100 ± 770	0.715
764.80	−5400 ± 350	0.771
765.88	−3800 ± 350	0.905
766.86	− 200 ± 340	0.027
768.00	+3400 ± 270	0.169
768.95	+4200 ± 280	0.288
769.96	+3400 ± 280	0.414
770.80	+1300 ± 280	0.514
771.03	+ 370 ± 250	0.547

giving the Julian date at the midpoint of the observation, the measured effective field H_e and its standard error σ_H, and the phase ϕ of the observation (determined as described below).

Two recent ephemerides are available for 53 Cam. Preston and Stępień (1968) adopt a period of 8d0278 based on eight magnetic measurements made at Lick in 1965 and 1967 and Babcock's (1958) 11 published observations from 1957, and on photometry. Babcock gives a period of 8d0269 based on a very well defined magnetic curve containing 61 measurements made between 1957 and 1961, most of which are unpublished (Huchra 1972). When our data are compared with those of Babcock and of Preston and Stępień, it appears that a slightly shorter period gives the most satisfactory representation of all of the magnetic data. If we adopt the elements

$$\text{JD (positive crossover)} = 2{,}435{,}855.652 + 8.0267E, \quad (4)$$

the data of Babcock given by Huchra (1972) are altered in phase by less than 0.01, the general agreement between Babcock's magnetic curve and the data of Preston and Stępień (1968) is improved, and the points of phase reflection symmetry in our magnetic curve coincide closely with those of Babcock. We estimate that the uncertainty in this period is ~0d0002. Phase in Table 1 is therefore computed from the elements of equation (4).

For α^2 CVn, the photographically observed magnetic curve is rather asymmetric and depends to some extent on the element measured (Pyper 1969). We find that when our data are plotted on the ephemeris of Farnsworth (1932):

$$\text{JD (Eu II maximum)} = 2{,}419{,}869.720 + 5.46939E, \quad (5)$$

the magnetic curve appears to be $\lesssim 0.02$ in phase out from the curves of Babcock (1960) and Pyper (1969). We have not attempted to improve this period.

TABLE 2

Hβ MAGNETOGRAPH OBSERVATIONS OF α^2 CANUM VENATICORUM

JD (2,442,000+)	$H_e \pm \sigma_H$ (gauss)	ϕ
495.85	− 460 ± 140	0.865
496.81	−1300 ± 100	0.041
498.74	+ 750 ± 130	0.394
499.02	+ 850 ± 290	0.445
499.64	+1200 ± 290	0.558
500.69	− 520 ± 110	0.750
501.02	− 990 ± 100	0.811
501.70	−1200 ± 110	0.935
502.02	−1400 ± 100	0.993
502.77	−1060 ± 130	0.131
503.02	− 720 ± 120	0.176
519.73	− 270 ± 130	0.231
543.79	+ 290 ± 160	0.631
592.64	+ 730 ± 110	0.562
767.05	+ 940 ± 55	0.450
768.06	+ 470 ± 65	0.635
769.02	− 940 ± 65	0.811
770.01	−1330 ± 75	0.991
850.76	− 560 ± 110	0.756
857.71	−1080 ± 95	0.026
920.61	+ 770 ± 100	0.527

III. COMPARISON OF PHOTOGRAPHIC AND PHOTOELECTRIC MEASUREMENTS

The magnetic field measurements of Tables 1 and 2 are plotted against the phase in Figures 1 and 2. Figure 1 shows all Hβ data for 53 Cam, compared with a smoothed representation of Babcock's photographic field curve (Huchra 1972). Figure 2 shows the new Hβ

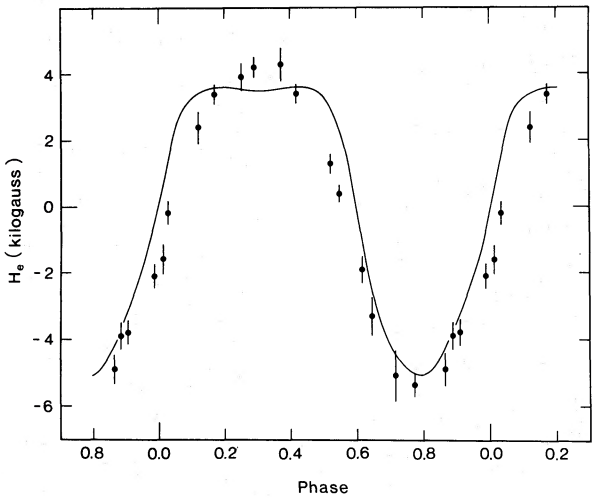

FIG. 1.—Hβ magnetograph observations (*filled circles*) of the magnetic field of 53 Cam plotted against phase. Error bars indicate ±1 standard error. The smooth curve is a freehand average of Babcock's photographic magnetic curve.

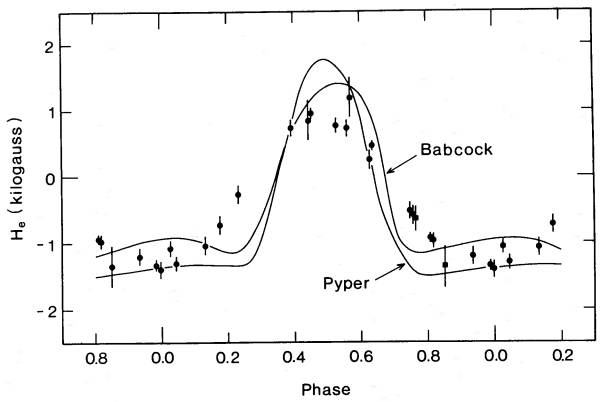

FIG. 2.—Hβ (*filled circles*) and Hα (*filled squares*) magnetograph observations of α^2 CVn plotted against phase. The two smooth curves are freehand representations of Babcock's and Pyper's photographic magnetic curves.

measurement of α^2 CVn together with two Hα measurements from Landstreet *et al.* (1975). These data are compared with Babcock's (1960) photographic magnetic curve, and with the mean of the three magnetic curves measured by Pyper (1969) for her element groups 1, 2, and 3 (respectively rare earths, iron peak elements, and other elements).

It is clear from Figures 1 and 2 that the photoelectric Hβ magnetic curves are much more nearly sinusoidal than those measured photographically. The broad plateaus present in photographic curves of both 53 Cam and α^2 CVn are gone. In view of the considerable discordance between the two types of magnetic curves, we must consider which type more nearly corresponds to the quantity H_e usually calculated from model geometries for comparison with observation.

The photographic magnetic curves are determined from metal absorption lines. In the case of spectrum variables, which have a nonuniform distribution of some elements over the stellar surface, the net measured longitudinal magnetic field is weighted by local equivalent width, and thus does not necessarily correspond at all closely to H_e. Of the two stars considered here, α^2 CVn is an outstanding spectrum variable which apparently has variations in local iron-peak and rare-earth abundances of at least a factor of several over the photosphere (Pyper 1969). Spectrum variations are also reported in 53 Cam (Babcock 1958), but according to Preston (private communication) visual inspection of a number of plates shows that the variations of Fe and Cr (which dominate the spectrum) are mainly due to variable magnetic intensification, while abundance variations are mild if they are present at all. The lines of Ti II show much larger variations, probably due to a nonuniform distribution of Ti, but this element contributes only a small fraction of the lines measured for He, so that its nonuniform distribution does not affect the measured effective field very much. Thus the photographic magnetic curve of α^2 CVn may not correspond very closely to H_e, while in the case of 53 Cam it appears that patchiness is not very important. In contrast, the photoelectric Hβ curves are measured using hydrogen, an element which is expected to be distributed uniformly, so that the nonuniform weighting problem does not arise.

In addition, it was shown in Paper I that the photographic field measuring technique commonly used is subject to systematic errors which arise because of the complex shapes of the circularly analyzed line profiles, the nonlinearity of the photographic emulsion, and the necessity of having a human being estimate visually the centroid of line components. These problems are especially severe near crossover, which in many Ap stars occupies most of the cycle. These difficulties do not arise in our photoelectric measurements. The broad Balmer lines observed through 5 Å filters show no significant crossover effect, the measurements are linear, and the technique is entirely impersonal.

We conclude that the photoelectric Balmer line magnetic measurements are in all likelihood much closer to the theoretical quantity H_e than are photographic measurements in cases where the two disagree.

We must next consider the appropriate magnetic geometry for modeling our observations. As discussed in § I, interpreting the observations on the oblique rotator model leads to the conclusion in general that the stellar geometry is approximately dipolar in nature. In some cases one pole is stronger than the other, which is conveniently represented by the decentered-dipole model (Landstreet 1970; Wolff and Wolff 1970). The main difficulty with this model has been the extreme displacement ($a \gtrsim 0.5$) required to fit the very anharmonic H_e curves obtained photographically, which is inconsistent with the small variation in H_s observed for the few stars (53 Cam among them) for which H_s curves are available (Huchra 1972). In addition, with $a \gtrsim 0.5$ it is unlikely that the strong pole, which produces the sharp and narrow extremum in the calculated model H_e curve, would be detected by the photographic observer, as the contribution of this pole to the analyzed line profile is shallow and strongly displaced from the main line (Borra 1974*a*). In other words, a strongly decentered-dipole model leads to theoretical H_e curves which resemble those observed in α^2 CVn and 53 Cam, but it is unlikely that the photographic observer, observing a star with this field distribution, would actually measure an H_e curve at all like the theoretical one. With the new observations, we expect these problems to be much less severe. We shall therefore investigate below the extent to which the observations may be satisfactorily represented by a decentered dipole geometry.

IV. 53 CAMELOPARDALIS

We fit a decentered-dipole model to the photoelectric H_e and the photographic H_s data by using observed extrema $H_e^{\pm}$ and $H_s^{\pm}$ to determine the values of i, β, H_p, and a. For convenience, we take i to be less than 90°, β to be the angle between the observable stellar rotational pole and the positive magnetic pole, H_p to be the field value at the strong magnetic pole, and a to be the fractional displacement in the direction of the positive pole. This fitting may conveniently be

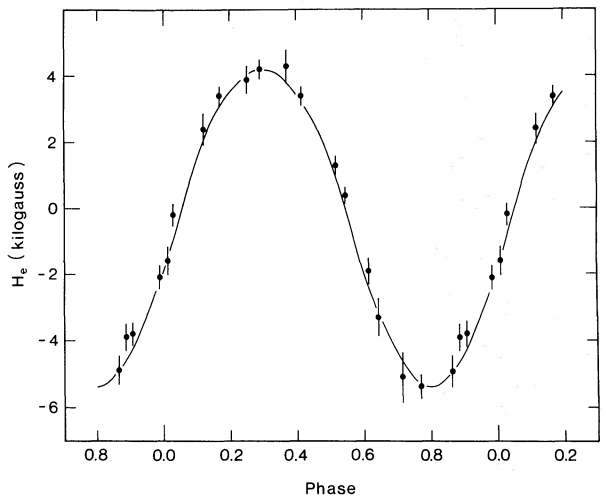

FIG. 3.—Comparison of magnetograph observations (*filled circles*) of 53 Cam with the effective magnetic field curve predicted by the model discussed in the text.

done with Preston's (1970) calculations of H_e and H_s for dipoles of various decentering parameters. This procedure leads to the parameters $(i, \beta, H_p, a) = (65°, 100°, -28{,}000 \text{ gauss}, -0.15)$ or $(80°, 115°, -28{,}000, -0.15)$. Because the extreme values $H_e^{\pm}$ measured by us are quite close to those observed photographically by Babcock, our model is very similar to the one derived by Huchra (1972), namely, $(i, \beta, H_p, a) = (50°, 100°, -28{,}400, -0.145)$.

The main uncertainty in our data is in the conversion of $\langle V \rangle$ to H_e. If we assume that our conversion is in error by 10%, all of the model parameters also change by about 10%, so we may reasonably regard them as being determined to about that accuracy.

The variation in H_e calculated for our model is compared with the new photoelectric field measurements in Figure 3. The fit to the data is extremely good. As our model is almost identical to Huchra's (1972), the theoretical H_s curve is not changed significantly from the one shown in his Figure 1, which is also an acceptable fit. It thus appears that the main difficulty in modeling the magnetic field of 53 Cam with a decentered dipole has disappeared, and in fact the model seems to be quite successful.

To investigate somewhat further the possibility of interpreting the photographic measurements, we have calculated theoretical photographic magnetic curves using the simple model discussed in Paper I. In this model, the Stokes parameters across a line profile are calculated for a triplet line formed in a Milne-Eddington model atmosphere (Unno 1956) as a function of position on the visible hemisphere of the star. The profiles are locally Doppler-shifted in accordance with the star's rotation and integrated over the disk. From the variation of the Stokes parameters across the line the circularly analyzed line profiles are calculated and convolved with a photographic characteristic curve. When the separation between the centroids of the right and left circularly analyzed line profiles is calculated, it generally gives a good measurement of the model's actual H_e value. However, it is argued in Paper I that in measuring a plate the observer tends to emphasize the cores of the analyzed profiles, especially when these profiles are complex, at the expense of the shallow wings. This effect is crudely modeled by calculating the centroids of the deepest 30% of the analyzed line profiles and converting their separation into a field measurement H_e^3. The field H_e^3 thus gives an indication, albeit a rather approximate one, of the field that would be measured by an observer from a photographic plate if he emphasized very strongly the line cores. The effect of less severe emphasis on line cores is modeled by calculating the separation of the centroids of the deepest 70% of the analyzed line profiles, which give the field measurement H_e^7.

We have calculated H_e^3 and H_e^7 magnetic curves for our model of 53 Cam. These are compared in Figure 4 with Babcock's observations. It is seen that the H_e^3 and H_e^7 curves model the photographic observations reasonably well near crossover but give fields which are much too large near the extrema. From this we conclude that the photographic observer probably does tend to emphasize the cores of the analyzed line profiles somewhat near crossover, but that his measurements are more successful near field extrema where the line profiles are simpler. It is notable, in fact, how well the photoelectric and photographic measurements agree near the field extrema, differing by less than the uncertainty in the scale of the photoelectric measurements.

The agreement between the photoelectric and photographic field measurements near the field extrema also suggests that the photographic field measurements of H_s are reasonably accurate, as the (unanalyzed) Zeeman σ component profiles are expected to be relatively symmetric and simple.

Thus in 53 Cam, where variations in metal abundance across the visible disk are probably insignificant, we have evidence for the occurrence of the type of systematic error in the photographic measurements which was predicted in Paper I. As expected, these errors appear to be considerably more serious near crossover than at the extrema.

V. α^2 CANUM VENATICORUM

For this star the projected rotation velocity is too large to allow measurement of H_s, so that a unique decentered dipole model cannot be chosen. Instead, we shall estimate the value of i, using equation (1), and then use H_e^+ and H_e^- to determine β and H_p for decentered dipole models having a range of decentering parameter a. The resulting magnetic curves will be compared with our data to determine the acceptable range in a.

Preston (1971*b*) gives $v_e \sin i = 24 \text{ km s}^{-1}$ for α^2 CVn, while Abt *et al.* (1972) give 18 km s^{-1}. This is perhaps a reasonable indication of the uncertainty of the value. Now, to determine i from equation (1) we must estimate R. The hydrogen spectral type of α^2 CVn

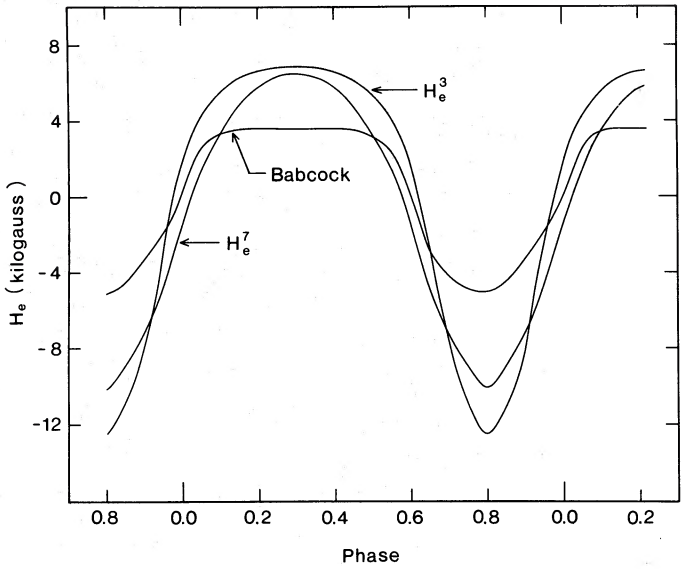

FIG. 4.—Comparison of Babcock's photographic magnetic curves with the model photographic curves H_e^3 and H_e^7

is B7 (Osawa 1965) and the zero-age main-sequence (ZAMS) radius at this spectral type (cf. Code *et al.* 1976) is $R_{\rm ZAMS} = 1.9\ R_\odot$. This leads to a maximum i of 90°. During the main-sequence lifetime of the star its radius increases by a factor of about 2. With $v_e \sin i \geqslant 18$ km s^{-1} and $R \leqslant 3.8\ R_\odot$, we find $i \geqslant 30°$. Taking $R \sim 1.5 R_{\rm ZAMS}$ as a reasonable guess and using Preston's value of $v_e \sin i$ (because of the higher dispersion on which it is based) we arrive at an estimate of $i \approx 65°$, which we shall assume below. This agrees reasonably well with the value of $i = 50°$ determined by Pyper (1969) in her study of the spectrum variations of α^2 CVn.

We then use the observed extreme values of H_e, H_e^+, and H_e^-, together with Preston's (1970) curves of $H_e(\alpha)$ (where α is the angle between the line of sight and the strong magnetic pole) to find the angles $\alpha_1 = \beta + i$ and $\alpha_2 = \beta - i$ such that $H_e(\cos \alpha_1)/H_e(\cos \alpha_2) = H_e^-/H_e^+ = -1.35$, with $i = 65°$. This is carried out for $a = 0.0$, 0.2, and 0.4, and assumes that the strong pole is the positive pole, which is in view near phase 0.5, when the sharp photographic extremum occurs. The resulting model parameters are $\beta = 109°$ and $H_p = 4400$ gauss for $a = 0.0$, and $\beta = 115°$ and $H_p = 10{,}000$ gauss for $a = 0.2$. For $a = 0.4$, i must be reduced to 60° to allow a model; in this case $\beta = 117°$ and $H_p = 26{,}700$ gauss. To see how sensitive the shapes of the H_e curves are to the choice of i, we have repeated the procedure above for $i = 40°$, 60°, and 90°. The H_e curves predicted at a given a are virtually indistinguishable for i in this range except for a slight difference between the curves at $a = 0.4$ with $i = 40°$ and 60°. In these models, β is in the range of 90°–140°. In Figure 5 we compare our observations of α^2 CVn with the H_e curves for $i = 65°$ and $a = 0.0$; $i = 65°$ and $a = 0.2$; and $i = 60°$, $a = 0.4$. It appears that

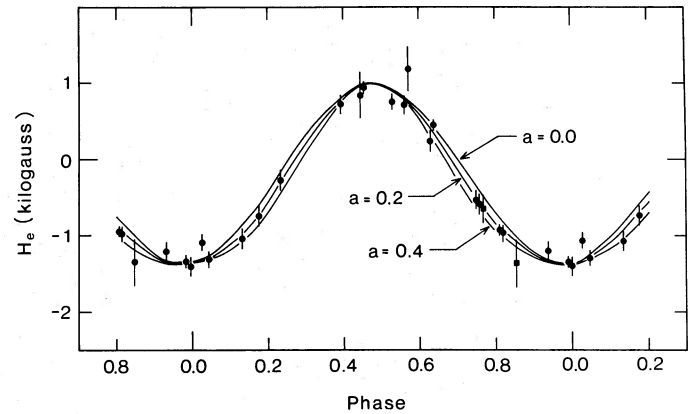

FIG. 5.—Comparison of magnetograph observations (*filled circles* and *squares*) of α^2CVn with the effective magnetic field curves for the models (i, β, H_p, a) = (65°, 109°, 4400, 0.0), (65, 115°, 10,000, 0.2), and (60°, 117°, 26,700, 0.4). The model curves are labeled by the values of a. H_e^+ occurs at $\phi = 0.48$ for the theoretical curves.

$a = 0.2$ is the best fit, although values of $a = 0.0$ and 0.4 would be acceptable. The curve with $a = 0.4$ and $i = 40°$ lies between the curves shown in Figure 5 for $a = 0.2$ and $a = 0.4$.

We are thus unable to choose a unique model for α^2 CVn with the available information, but we may conclude that our magnetic data are consistent with decentered-dipole models having small to moderate decentering ($a \lesssim 0.4$), large obliquity, and reasonable values of H_p (between 4400 and 27,000 gauss).

It is instructive to compare our models with the field distribution found by Pyper (1969). Her final field distribution is qualitatively rather similar to a decentered-dipole model with the parameters (50°, 55°, 20,000, 0.26). It thus differs from our models mainly in having the observer's line of sight pass almost directly over the strong positive pole, while in our models the line of sight passes nearer to the weaker negative pole. The H_e curve obtained from Pyper's model for a uniformly distributed element is shown in her Figure 16; it is nearly sinusoidal with $H_e^+ = 1.7$ kilogauss and $H_e^- = -0.7$ kilogauss. In contrast, the observed magnetograph H_e curve (Fig. 2) has $H_e^+ = 1.0$ kilogauss and $H_e^- = -1.35$ kilogauss. With our observed values of H_e^+ and H_e^-, the positive pole can pass nearer the line of sight than the negative pole only if the negative pole is considerably stronger ($a \lesssim -0.2$) than the positive pole. In this case, however, our observed magnetic curve would have a narrower negative extremum and a broader positive extremum than the $a = 0.0$ curve in Figure 5, and this is not observed. In addition, we would not be able to account for the shape of the photographic magnetic curves (see below). Thus, although our magnetic geometry is not very well specified ($i \gtrsim 30°$, $90 \lesssim \beta \lesssim 140°$, $0.0 \lesssim a \lesssim 0.4$) it appears to be unambiguously different from that inferred by Pyper from her H_e curves. With our magnetic geometry, the four iron-peak patches do not lie along the magnetic equator, and the rare-earth patch is no longer nearly concentric with the negative magnetic pole. However, it is difficult to assess the uniqueness of Pyper's equivalent width distributions, and further work clarifying this point would be very helpful in establishing the relationship between the magnetic geometry and the photospheric distribution of material.

The nonuniform distribution of elements may be significant in determining the shape of the observed H_e curve. This is suggested by the fact that the H_e curves calculated by Pyper from her magnetic model for the rare-earth (group 1) and iron-peak (group 2) distributions that she derived lead to H_e curves similar to her observed magnetic curve (cf. Fig. 2), and quite different from the calculated H_e curve of a uniformly distributed element. However, nonuniformity may not be the dominant effect in leading to the shapes of Pyper's magnetic curves, as her observed magnetic curves for all three groups of elements, with their rather different surface distributions, are quite similar. We have calculated H_e^3 and H_e^7 curves for our best model, which are compared with Pyper's photographic observations in Figure 6. The H_e^7 curve actually reproduces Pyper's observations rather well, although in view of the strong nonuniformity of the metal distribution on this star the agreement is perhaps fortuitous. Because of the difficulties in the interpretation of photographic field measurements it would appear worthwhile to obtain high-resolution photoelectric field measurements of α^2 CVn from metal lines (using the technique of Borra, Landstreet, and Vaughan (1973), for example) to test our model. Such observations have recently been obtained, and the data are currently being analyzed. Preliminary results for two lines of Fe II give fairly sinusoidal field curves with $H_e^+ \sim +1$ kilogauss and $H_e^- \sim -1$ kilogauss, so that our field measurements for iron seem more nearly like our Balmer-line field measurements than the Pyper group 2 magnetic curve, again supporting the view that the

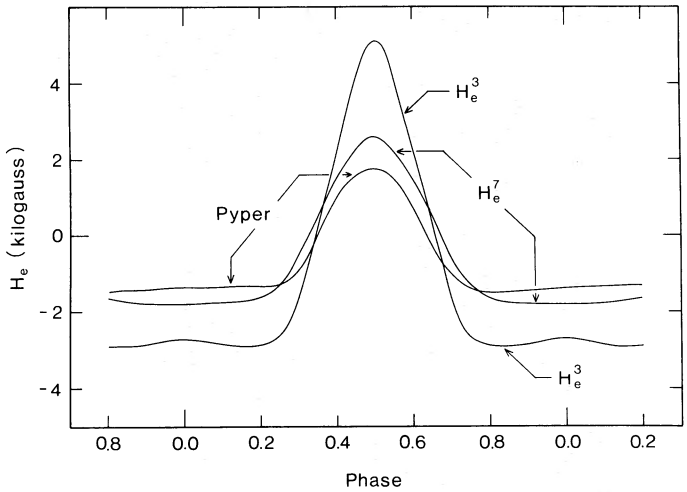

FIG. 6.—Comparison of Pyper's photographic magnetic curve with the model photographic curves H_e^3 and H_e^7 calculated for the model $(i, \beta, H_p, a) = (65°, 115°, 10{,}000, 0.2)$.

shape of the photographic magnetic curves is strongly affected by the effects discussed in Paper I.

VI. CONCLUSIONS

We may summarize the conclusions of this paper as follows. The photoelectric and photographic magnetic curves of 53 Cam and α^2 CVn are quite different from one another (although the extreme values observed for the field, $H_e^{\pm}$, are quite similar). We believe that the photoelectric magnetic curves are close to the theoretical H_e curves easily computed from model field distributions. In contrast, the photographic magnetic curves seem to be subject to the measurement errors discussed in Paper I, and may also in the case of α^2 CVn be significantly affected by nonuniform metal distribution. Our photoelectric H_e curves for 53 Cam and α^2 CVn are in very satisfactory agreement with the predictions of decentered-dipole models. A unique model appears to fit all the magnetic observations of 53 Cam, while the observations of α^2 CVn may be accounted for by a reasonable family of models.

Further photoelectric observations of the magnetic curves of other magnetic stars may be expected to be useful in modeling, both because such observations allow the problem of determining the field distribution to be decoupled from the problem of finding the distribution of elements over the surface of the star, and because the photoelectric measurements are free of the measurement reduction difficulties discussed above. Such observations are currently being obtained for several of the brighter magnetic stars.

We are grateful to the director of the Hale Observatories for generous grants of observing time at Mount Palomar and Mount Wilson Observatories. The work has been supported by the National Research Council of Canada.

REFERENCES

Abt, H. A., Chaffee, F. H., and Suffolk, G. 1972, *Ap. J.*, **175**, 779.
Angel, J. R. P., and Landstreet, J. D. 1970, *Ap. J. (Letters)*, **160**, L147.
Babcock, H. W. 1958, *Ap. J. Suppl.*, **3**, 141.
———. 1960, in *Stellar Atmospheres*, ed. J. L. Greenstein (Chicago: University of Chicago Press), p. 382.
Borra, E. F. 1974*a*, *Ap. J.*, **187**, 271.
———. 1974*b*, *Ap. J.*, **188**, 287 (Paper I).
Borra, E. F., and Landstreet, J. D. 1975, *Pub. A.S.P.*, **87**, 961.
Borra, E. F., Landstreet, J. D., and Vaughan, A. H. 1973, *Ap. J. (Letters)*, **185**, L145.
Code, A. D., Davis, J., Bless, R. C., and Hanbury Brown, R. 1976, *Ap. J.*, **203**, 417.
Farnsworth, G. 1932, *Ap. J.*, **76**, 313.
Huchra, J. 1972, *Ap. J.*, **174**, 435.
Landstreet, J. D. 1970, *Ap. J.*, **159**, 1001.
Landstreet, J. D., Borra, E. F., Angel, J. R. P., and Illing, R. M. E. 1975, *Ap. J.*, **201**, 624.
Osawa, K. 1965, *Ann. Tokyo Astr. Obs.*, Ser. 2, **9**, 123.
Preston, G. W. 1969, *Ap. J.*, **157**, 247.
———. 1970, *Ap. J.*, **160**, 1059.
———. 1971*a*, *Pub. A.S.P.*, **83**, 571.
———. 1971*b*, *Ap. J.*, **164**, 309.
Preston, G. W., and Stępień, K. 1968, *Ap. J.*, **151**, 583.
Pyper, D. 1969, *Ap. J. Suppl.*, **18**, 347.
Stibbs, D. W. N. 1950, *M.N.R.A.S.*, **110**, 395.
Unno, W. 1956, *Pub. Astr. Soc. Japan*, **8**, 108.
Wolff, S. C., and Wolff, R. J. 1970, *Ap. J.*, **160**, 1049.

ERMANNO F. BORRA: Département de Physique, Université Laval, Québec, Québec, Canada

J. D. LANDSTREET: Department of Astronomy, University of Western Ontario, London, Ontario, Canada, N6A 5B9